

A Thermodynamic Study on the Binding of Cobalt(II) and Iron(III) Ions with Bovine Carbonic Anhydrase II at Different Temperatures

G. Rezaei Behbehani · A. Divsalar · A.A. Saboury ·
R. Hajian · Z. Rezaei · E. Yahaghi · L. Barzegar

Received: 12 August 2009 / Accepted: 22 March 2010 / Published online: 26 August 2010
© The Author(s) 2010. This article is published with open access at Springerlink.com

Abstract A thermodynamic study on the interaction of bovine carbonic anhydrase II, CAII, with cobalt(II) and iron(III) ions was made using isothermal titration calorimetry (ITC) at 300.15 K and 310.15 K in Tris buffer solutions at pH = 7.5. The enthalpies of interaction of Co^{2+} + CAII and Fe^{3+} + CAII are reported and analyzed in terms of the extended solvation theory. The results indicate that there are three identical and non-cooperative binding sites for Co^{2+} and Fe^{3+} ions. Binding of these ions with CAII occurs exothermically with dissociation equilibrium constants of 87.15 and 91.00 $\mu\text{mol}\cdot\text{L}^{-1}$ at 300.15 K, for Co^{2+} and Fe^{3+} , respectively.

Keywords Bovine carbonic anhydrase · Cobalt ion · Isothermal titration calorimetry

1 Introduction

Carbonic anhydrases, CA, are ubiquitous zinc enzymes that are present in archaea, prokaryotes and eukaryotes, which are encoded by three distinct, evolutionarily unrelated, genetic

G. Rezaei Behbehani (✉)
Chemistry Department, Imam Khomeini International University, Qazvin, Iran
e-mail: grb402003@yahoo.com

A. Divsalar · A.A. Saboury
Institute of Biochemistry and Biophysics, University of Tehran, Tehran, Iran

A. Divsalar
Department of Biological Sciences, Tarbiat Moallem University, Tehran, Iran

R. Hajian · Z. Rezaei
Department of Chemistry, Islamic Azad University, Gachsaran, Iran

E. Yahaghi
School of Chemistry, University of Tehran, Tehran, Iran

L. Barzegar
Department of Chemistry, Payam Noor University (PNU), Abhar, Iran

families, and occur as α -CA, β -CA and γ -CA forms [1–4]. CA is one of the fastest acting enzymes known, with a maximal turnover rate for CO_2 hydration of $\sim 10^6 \text{ s}^{-1}$ at 25°C , which is probably the reason why the activation of CA has not been much studied. In contrast, inhibition of CA has been widely investigated and crystal structures have been reported of several CA complexes with inhibitor molecules [1, 5].

CAII is a novel metallo protein due to its unusually high affinity for zinc(II), whose CAII + Zn^{2+} dissociation constant is $1\text{--}10 \text{ pmol}\cdot\text{L}^{-1}$ [1]. The role of highly conserved aromatic residues surrounding the zinc-binding site of human carbonic anhydrase II (CAII), in determining the metal ion binding specificity of this enzyme, has been previously examined using mutagenesis [6, 7]. Residues F93, F95, and W97 are located along a β -strand containing two residues that coordinate zinc, H94 and H96, and these aromatic amino acids contribute to the high zinc affinity and slow rate constant for dissociation of Zn(II) from CAII. Substitution of these aromatic amino acids with smaller side chains enhances the affinity for copper (up to 100 fold) while decreasing the affinity for both cobalt and zinc, thereby altering the metal ion binding specificity by as much as a factor of 10^4 . Furthermore, the Gibbs energy for stabilization of native CAII, determined by solvent-induced denaturation, correlates positively with the increased hydrophobicity of the amino acids at positions 93, 95, and 97, as well as with affinities for Co(II) and Zn(II) [8, 9]. Conversely, an increased affinity for Cu(II) correlates with decreased protein stability. Although CAII is loaded with Zn(II) in its physiologically relevant condition, it can also bind a number of other divalent metal ions at the zinc binding site including Co^{2+} , Ni^{2+} , Cu^{2+} , Cd^{2+} , Hg^{2+} and Pb^{2+} but with different affinities [4, 7].

Some Zn(II) and Cu(II) metal complexes of sulfonamides that incorporate polyamino-polycarboxylated tails have also been reported, which indeed show very good in vitro inhibitory activity against the isoforms CA I, II, and IV [7, 8]. In this paper, the effects of Co(II) and Fe(III) ions on the structure and stability of CAII are examined.

2 Materials and Method

Erythrocyte bovine carbonic anhydrase was obtained from Sigma. Copper sulfate was obtained from Merck. The buffer solution used in the experiments, which was $50 \text{ mmol}\cdot\text{L}^{-1}$ Tris, pH = 7.5, was obtained from Merck.

All of the calorimetry experiments were carried out in 300.15 K and 310.15 K. The experiments were performed with a 4-channel commercial microcalorimetric system, Thermal Activity Monitor 2277 (Thermometric, Sweden). Each channel is a twin heat-conduction calorimeter (multijunction thermocouple plates), positioned between the vessel holders and the surrounding heat sink. Both sample and reference vessels are made from stainless steel. The limiting sensitivity of the calorimeter is $0.4 \mu\text{J}$. Cobalt(II) nitrate solution ($5 \text{ mmol}\cdot\text{L}^{-1}$) was injected by use of a Hamilton syringe into the calorimetric titration vessel, which contained 1.8 mL of $30 \text{ }\mu\text{mol}\cdot\text{L}^{-1}$ CA solution, in the Tris buffer ($30 \text{ mmol}\cdot\text{L}^{-1}$) at pH = 7.5. Thin (0.15 mm inner diameter) stainless steel hypodermic needles, permanently fixed to the syringe, reach directly into the calorimetric vessel. Injection of $20 \mu\text{L}$ metal nitrate samples into the perfusion vessel was repeated 30 times. The calorimetric signal was measured with a digital voltmeter that was part of a computerized recording system. The heat of injection was calculated with the “Thermometric Digitam 3” software program. The heats of dilution of Co(II) and Fe(III) nitrate solution were measured as described above except that CAII was absent. Also, the enthalpy of dilution of the protein solution was measured as described above, except that buffer solution was injected into the protein solution in the sample cell. The enthalpies of dilution of $\text{Co}(\text{NO}_3)_2$, $\text{Fe}(\text{NO}_3)_3$ and protein solutions were subtracted

Table 1 The heats of Co^{2+} + CAII interactions, q , at 300 K and 310 K, where the q_{dilut} are heats of dilution of $\text{Co}(\text{NO}_3)_2$ with water. The precision of the measurements is $\pm 0.1 \mu\text{J}$ or better

[Co^{2+}]/mM	[CAII]/ $\mu\text{mol}\cdot\text{L}^{-1}$	$q^{\text{a}}/\mu\text{J}$	$q_{\text{dilut}}^{\text{a}}/\mu\text{J}$	$q^{\text{b}}/\mu\text{J}$	$q_{\text{dilut}}^{\text{b}}/\mu\text{J}$
0.055	29.670	-635.3	-424.8	-563.5	-398.3
0.109	29.348	-1065.4	-790.4	-954.2	-742
0.161	29.032	-1350.6	-1089.6	-1222.6	-1021.5
0.213	28.723	-1543.7	-1344	-1410.7	-1260
0.263	28.421	-1679.4	-1562.4	-1546.7	-1464.7
0.312	28.125	-1778.5	-1740	-1648.3	-1631.2
0.361	27.835	-1853.4	-1895.2	-1726.5	-1776.7
0.408	27.551	-1911.7	-2028.8	-1788.2	-1902
0.454	27.273	-1958.2	-2140.8	-1838	-2008
0.500	27.000	-1996.1	-2232	-1879	-2092.5
0.544	26.733	-2027.6	-2316.5	-1913.2	-2171.3
0.588	26.470	-2054.1	-2390.1	-1942.2	-2240.3
0.631	26.214	-2076.7	-2456.5	-1967.1	-2302.5
0.673	25.962	-2096.2	-2510.9	-1988.6	-2353.5
0.714	25.714	-2113.2	-2561.8	-2007.4	-2401.7
0.755	25.472	-2128.1	-2605	-2024	-2442.2
0.794	25.233	-2141.3	-2644.8	-2038.8	-2479.7
0.833	25.000	-2153.1	-2681.6	-2052	-2513.2
0.872	24.771	-2163.7	-2715.2	-2063.9	-2544.7
0.909	24.545	-2173.2	-2745	-2074.6	-2572.4
0.946	24.324	-2181.8	-2771.4	-2084.3	-2597.2
0.982	24.107	-2189.7	-2794.8	-2093.2	-2618.9
1.018	23.894	-2196.9	-2816.4	-2101.3	-2640.2
1.053	23.684	-2203.5	-2836.2	-2108.8	-2658.9
1.087	23.478	-2209.6	-2854.6	-2115.7	-2676.6
1.121	23.276	-2215.2	-2870.4	-2122.1	-2691.6

^aAt 300 K^bAt 310 K

from the heats of $\text{Co}(\text{NO}_3)_2$ and $\text{Fe}(\text{NO}_3)_3$ in CAII solutions. The measured heats for Co^{2+} + CAII and Fe^{3+} + CAII interactions are listed in Tables 1 and 3 (in μJ). The microcalorimeter was frequently calibrated electrically during the course of the study.

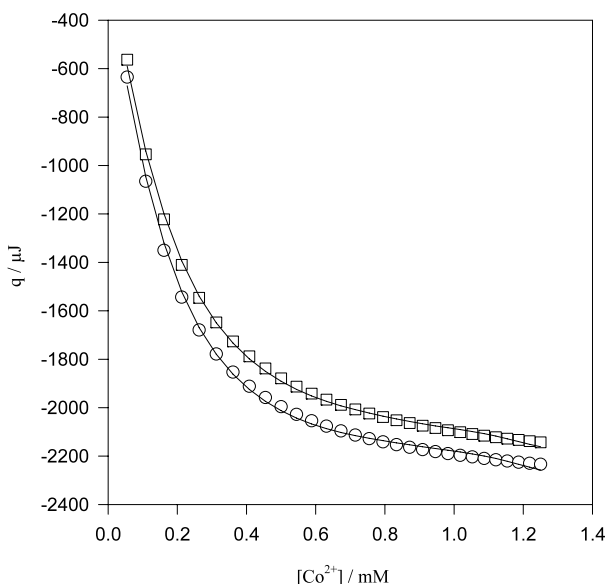
3 Results and Discussion

It has been shown previously [8–12] that the enthalpies of interaction of biopolymers with ligands in aqueous solutions can be reproduced with the following equation

$$q = q_{\max}x'_B - \delta_A^\theta(x'_A L_A + x'_B L_B) - (\delta_B^\theta - \delta_A^\theta)(x'_A L_A + x'_B L_B)x'_B \quad (1)$$

The parameters δ_A^θ and δ_B^θ are measures of the CAII stability as a result of interaction with a metal ion, L , at low and high metal ions concentration, respectively. If the binding of

Fig. 1 Comparison of the experimental heats for Co^{2+} + CAII interactions at 300 K (\circ) and 310 K (\square) with calculated results (lines) via Eq. 1; “mM” denotes concentration units of $\text{mmol}\cdot\text{L}^{-1}$



ligand at one site increases the affinity for this ligand at another site, then the macromolecule exhibits positive cooperativity. Conversely, if the binding of ligand at one site lowers the affinity for the ligand at another site, then the protein exhibits negative cooperativity. If the ligand binds at each site independently, then the binding is non-cooperative. Values of $p < 1$ or $p > 1$ indicate positive or negative cooperativity for binding of a macromolecule with metal ion ligand, respectively, whereas $p = 1$ indicates that the binding is non-cooperative. x'_B can be expressed as follows:

$$x'_B = \frac{px_B}{x_A + px_B} \quad (2)$$

where x'_B is the fraction of the metal ions (Co^{2+} or Fe^{3+}) bound to the sites on CAII, and $x'_A = 1 - x'_B$ is the fraction of the unbound (“free”) metal ions (L_F). We can express x_B in terms of the total metal ion concentration, L_T , divided by the maximum concentration of the metal ion upon saturation of all CAII binding sites, L_{\max} , as follows:

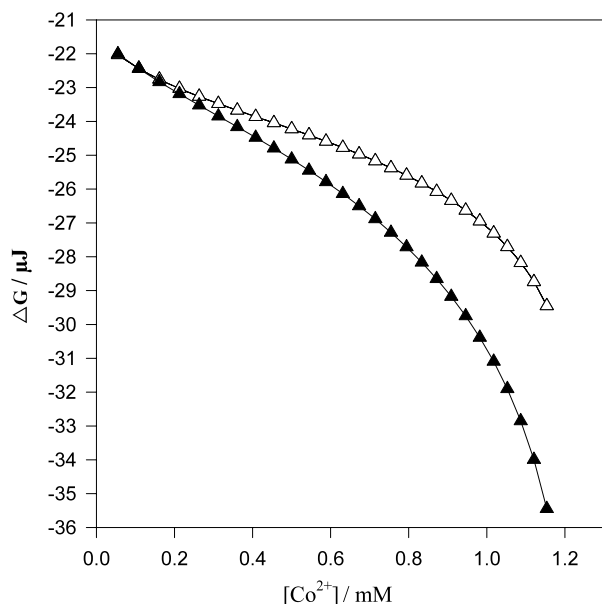
$$x_B = \frac{L_T}{L_{\max}}, \quad x_A = 1 - x_B \quad (3)$$

L_A and L_B are the relative contributions of unbound and bound Co^{2+} or Fe^{3+} to the enthalpies of dilution when CAII is absent and can be calculated from the enthalpies of dilution of Co^{2+} or Fe^{3+} in the buffer, q_{dilut} , as follows:

$$L_A = q_{\text{dilut}} + x_B \left(\frac{\partial q_{\text{dilut}}}{\partial x_B} \right), \quad L_B = q_{\text{dilut}} - x_A \left(\frac{\partial q_{\text{dilut}}}{\partial x_B} \right) \quad (4)$$

The heats of $L + \text{CAII}$ interactions, q , were fitted to Eq. 1. In the fitting procedure, only the adjustable parameter p was changed until the best agreement was obtained between the experimental and calculated data (Figs. 1 and 4). The optimized δ_A^θ and δ_B^θ values are recovered from the coefficients of the second and third terms of Eq. 1. The agreement between

Fig. 2 Comparison of experimental Gibbs energies at 300 K (Δ) and 310 K (\blacktriangle) for Co^{2+} + CAII interactions and calculated results (lines) via Eqs. 7 and 8; mM denotes concentration units of $\text{mmol}\cdot\text{L}^{-1}$. The linearity of ΔG as a function of the Co^{2+} concentration at lower concentrations indicates that the structural effects compensate each other in the Gibbs energy, which supports the extended solvation model



calculated and experimental results (Fig. 1) is excellent and gives considerable support to the use of Eq. 1.

Φ is the fraction of CAII molecules undergoing complexation with Co^{2+} or Fe^{3+} , which can be expressed as follows:

$$\Phi = \frac{q}{q_{\max}} \quad (5)$$

where q_{\max} represents the heat value obtained when all CAII binding sites are saturated. The apparent equilibrium constant, K_a , as a function of the free concentration of metal ion, L_F , is given by the following equation:

$$K_a = \frac{\Phi}{(1 - \Phi)L_F} = \frac{\Phi}{(1 - \Phi)L_T(1 - x_B)} \quad (6)$$

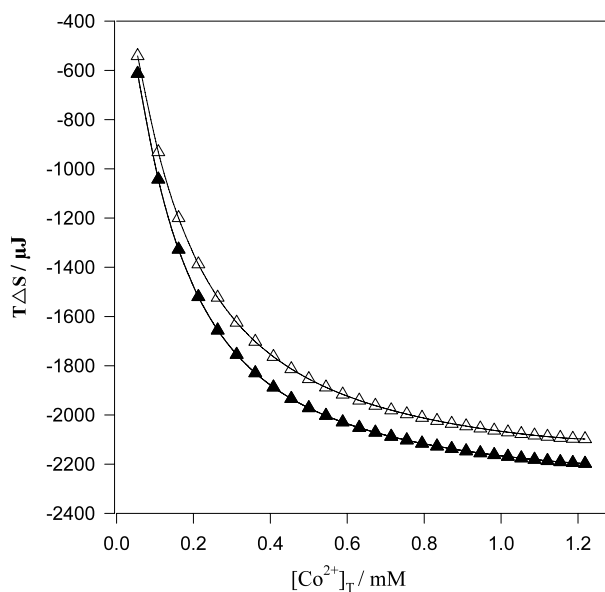
The Gibbs energies as a function of ligand concentrations can be calculated from:

$$\Delta G = -RT \ln K_a \quad (7)$$

Values of ΔG , calculated from Eq. 7 at different temperatures, are shown graphically in Figs. 2 and 5. The ΔS values were calculated from the ΔG values at different temperatures and are shown in Figs. 3 and 6. The linearity of ΔG against Co^{2+} and Fe^{3+} concentrations indicates that structural effects compensate each other in the Gibbs energy, which supports the use of the extended solvation model.

Consider a solution containing a ligand (Co^{2+} or Fe^{3+}) and a macromolecule (CAII in this case) that contains g sites capable of binding the ligand. If the multiple binding sites on a macromolecule are identical and independent, then the ligand binding sites can be analyzed by a model system of monomeric molecules $\{(CAII)_g \rightarrow g(CAII)\}$ having the same set of

Fig. 3 Comparison between the experimental entropies at 300 K (\blacktriangle) and 310 K (\triangle) for Co^{2+} + CAII interactions and calculated results (lines) via Eqs. 7 and 8; mM denotes concentration units of $\text{mmol}\cdot\text{L}^{-1}$



dissociation equilibrium constant, K_d , values. Thus, the reaction can be written as:

$$\text{M} + \text{L} \rightleftharpoons \text{ML} \quad K_d = \frac{[\text{M}][\text{L}]}{[\text{ML}]} \quad (8)$$

If α is defined as the fraction of free binding sites on the biomacromolecule, M_0 the total biomacromolecule concentration, and L_0 the total ligand concentration, then the free concentrations of monomeric molecule [M] and ligand [L] as well as the concentration of bound ligand [ML] can be deduced as follows:

$$[\text{ML}] = g(1 - \alpha)M_0 \quad (9)$$

$$[\text{L}] = L_0 - [\text{ML}] = L_0 - g(1 - \alpha)M_0, \quad (10)$$

$$[\text{M}] = gM_0 - [\text{ML}] = gM_0 - g(1 - \alpha)M_0 = \alpha g M_0 \quad (11)$$

Substitution of free concentrations of all these components in Eq. 8 gives:

$$K_d = \left(\frac{\alpha}{1 - \alpha} \right) L_0 - \alpha g M_0 \quad (12)$$

or

$$\alpha M_0 = \left(\frac{\alpha}{1 - \alpha} \right) \left(\frac{1}{g} \right) L_0 - \frac{K_d}{g} \quad (13)$$

Here $1 - \alpha$ is the fraction of occupied binding sites on the biomacromolecule:

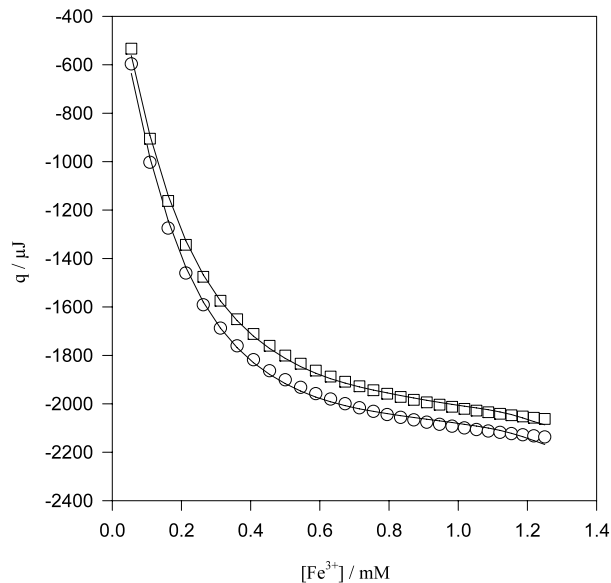
$$1 - \alpha = \frac{q}{q_{\max}} \quad (14)$$

where q represents the heat value at a certain ligand concentration L_0 , and q_{\max} represents the heat value upon saturation of all biomacromolecule with ligands. If q and q_{\max} are cal-

Table 2 Binding parameters for Co^{2+} –CAII interactions via Eq. 1. A value of $p = 1$ implies that Co^{2+} binds non-cooperatively to the native CAII structure. The positive values of δ_B^θ imply that specific interactions, defined here as preferential interactions between Co^{2+} ion and the native folded state of CAII, are dominant

Binding parameters	$T = 300.15 \text{ K}$	$T = 310.15 \text{ K}$
$K_1/\mu\text{mol}\cdot\text{L}^{-1}$	87.150 ± 0.016	105.084 ± 0.012
$K_2/\mu\text{mol}\cdot\text{L}^{-1}$	87.150 ± 0.016	105.084 ± 0.012
$K_3/\mu\text{mol}\cdot\text{L}^{-1}$	87.150 ± 0.016	105.084 ± 0.012
p	1 ± 0.004	1 ± 0.002
δ_A^θ	0.006 ± 0.001	-0.083 ± 0.016
δ_B^θ	3.680 ± 0.031	3.305 ± 0.021
$\Delta H_{\text{bin}}/\text{kJ}\cdot\text{mol}^{-1}$	-22.204 ± 0.034	-21.602 ± 0.012
g	3	3

Fig. 4 Comparison of the experimental heats for Fe^{3+} –CAII interactions at 300.15 K (○) and 310.15 K (□) and calculated results (lines) via Eq. 1; mM denotes concentrations in units of $\mu\text{mol}\cdot\text{L}^{-1}$



culated per mole of biomacromolecule, then the molar enthalpy of binding for each binding site (ΔH_{bin}) is given by:

$$\Delta H_{\text{bin}} = \frac{q_{\max}}{g}$$

Combining Eqs. 13 and 14 yields:

$$\left(\frac{\Delta q}{q_{\max}} \right) M_0 = \frac{\Delta q}{q} L_0 \left(\frac{1}{g} \right) - \frac{K_d}{g} \quad (15)$$

where $\Delta q = q_{\max} - q$. Therefore, a plot of $(\frac{\Delta q}{q_{\max}}) M_0$ versus $(\frac{\Delta q}{q}) L_0$ should be linear with a slope of $\frac{1}{g}$ and a vertical intercept of $\frac{K_d}{g}$.

Table 3 The heats of $\text{Fe}^{3+} + \text{CAII}$ interactions, q , at 300 K and 310 K, where the q_{dilut} are heats of dilution of $\text{Fe}(\text{NO}_3)_3$ with water. The precision is $\pm 0.1 \mu\text{J}$ or better

$[\text{Fe}^{3+}] / \mu\text{mol}\cdot\text{L}^{-1}$	$[\text{CAII}] / \mu\text{mol}\cdot\text{L}^{-1}$	$q^{\text{a}} / \mu\text{J}$	$q_{\text{dilut}}^{\text{a}} / \mu\text{J}$	$q^{\text{b}} / \mu\text{J}$	$q_{\text{dilut}}^{\text{b}} / \mu\text{J}$
54.945	29.670	-596.6	-382.6	-553.6	-358.7
108.696	29.348	-1002.8	-711.9	-905.4	-668.3
161.290	29.032	-1274.5	-981.5	-1162.5	-920.1
212.766	28.723	-1460	-1210.7	-1343.9	-1135.0
263.158	28.421	-1591.3	-1407.5	-1475.8	-1319.5
312.500	28.125	-1687.7	-1567.6	-1574.7	-1469.6
360.825	27.835	-1760.9	-1707.5	-1651.1	-1600.8
408.163	27.551	-1818	-1828	-1711.6	-1713.8
454.545	27.273	-1863.7	-1929.1	-1760.5	-1809.5
500.000	27.000	-1901	-2011.4	-1800.5	-1885.8
544.554	26.733	-1932	-2087.7	-1834.5	-1957.0
588.2352	26.470	-1958.2	-2154.2	-1863.1	-2019.5
631.068	26.213	-1980.5	-2214.2	-1887.7	-2075.6
673.077	25.961	-1999.8	-2263.4	-1909.0	-2121.8
714.286	25.714	-2016.6	-2309.5	-1927.6	-2165.4
754.717	25.472	-2031.4	-2348.6	-1944.1	-2202.2
794.392	25.234	-2044.5	-2384.7	-1958.7	-2236.2
833.333	25.000	-2056.2	-2418.1	-1971.8	-2266.6
871.559	24.770	-2066.7	-2448.6	-1983.6	-2295.2
909.091	24.545	-2076.2	-2475.7	-1994.2	-2320.4
945.946	24.324	-2084.8	-2499.7	-2003.9	-2343.0
982.143	24.107	-2092.6	-2521	-2012.7	-2362.8
1017.699	23.894	-2099.8	-2540.7	-2020.8	-2382.2
1052.631	23.684	-2106.4	-2558.8	-2028.2	-2399.3
1086.956	23.478	-2112.5	-2575.6	-2035.0	-2415.5
1120.690	23.276	-2118.1	-2590.1	-2041.3	-2429.3
1153.846	23.077	-2123.3	-2603.3	-2047.2	-2442.0
1186.441	22.881	-2128.1	-2614.4	-2052.7	-2452.4
1218.487	22.689	-2132.6	-2624.8	-2057.8	-2462.4
1250.000	22.500	-2136.8	-2633.7	-2062.6	-2470.9

^aAt 300 K^bAt 310 K

The linearity of the plot was examined by varying the estimated values for q_{\max} to yield a fit with the best value for the correlation coefficient. The best linear plot with the correlation coefficient value ($r^2 \approx 1$) was obtained using $-2398 \mu\text{J}$ and $-2333 \mu\text{J}$, equal to $-22.204 \text{ kJ}\cdot\text{mol}^{-1}$ and $-21.602 \text{ kJ}\cdot\text{mol}^{-1}$ at 300.15 K and 310.15 K, respectively. The values of g and K_d , obtained from the slope and vertical intercept of the plot are listed in Tables 2 and 4.

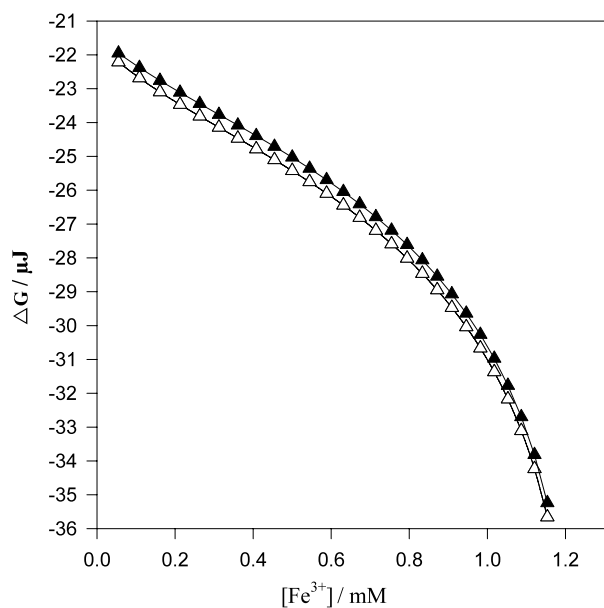
This calorimetric-based method described recently allows us to obtain the number of binding sites (g), the molar enthalpy of binding site (ΔH_{bin}), and the dissociation equilibrium constant (K_d) for a set of biomacromolecule binding sites. If no value for q_{\max} yields

Table 4 Binding parameters for Fe^{3+} + CAII interactions via Eq. 1. A value of $p = 1$ indicates that Fe^{3+} binding to CAII is non-cooperative. The positive values of δ_B^θ suggest that specific interactions, defined here as preferential interactions between Fe^{3+} and the native folded state of CAII, are dominant

Binding parameters ^a	$T = 300 \text{ K}$	$T = 310 \text{ K}$
$K_1/\mu\text{mol}\cdot\text{L}^{-1}$	91.009 ± 0.002	109.104 ± 0.002
$K_2/\mu\text{mol}\cdot\text{L}^{-1}$	91.009 ± 0.002	109.104 ± 0.002
$K_3/\mu\text{mol}\cdot\text{L}^{-1}$	91.009 ± 0.002	109.104 ± 0.002
p	1 ± 0.04	1 ± 0.05
δ_A^θ	0.010 ± 0.002	-0.076 ± 0.006
δ_B^θ	3.900 ± 0.027	3.532 ± 0.023
$\Delta H_{\max}/\text{kJ}\cdot\text{mol}^{-1}$	-47.335 ± 0.050	-46.337 ± 0.062
g	3	3

^aValues of K_1 , K_2 , and K_3 were assumed to be the same

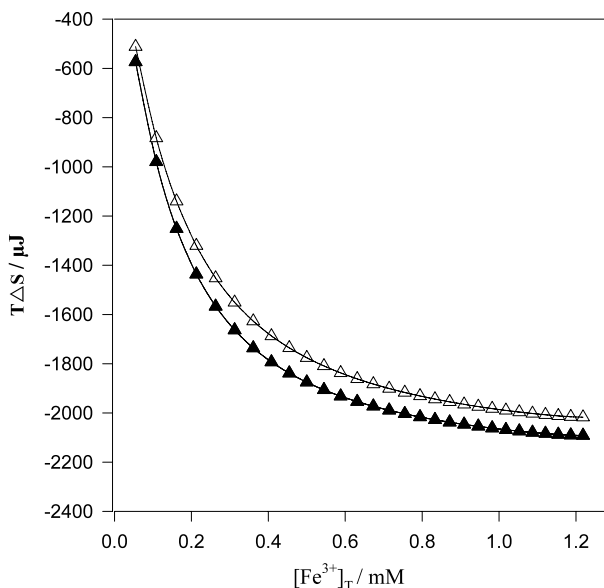
Fig. 5 Comparison between the experimental Gibbs energies at 300 K (\blacktriangle) and 310 K (\triangle) for Fe^{3+} + CAII interactions and calculated results (lines) via Eqs. 7 and 8; mM denotes concentrations in units of $\text{mmol}\cdot\text{L}^{-1}$. The linearity of ΔG against Fe^{3+} concentrations at lower concentrations indicates that structural effects compensate each other in the Gibbs energy, which supports the extended solvation model



a linear plot of $(\Delta q/q_{\max})M_0$ versus $(\Delta q/q)L_0$, then this may be attributed to the existence of non-identical binding sites or the interaction between them. Using this method shows that there are three identical and non-interacting binding sites for Co(II) ions.

Binding parameters for Co^{2+} + CAII and Fe^{3+} + CAII interactions, based on the extended solvation model, are listed in Tables 2 and 4. Similar values for K_q at all three identical binding sites points toward specific interactions between CAII and Co^{2+} or Fe^{3+} ions. Values of δ_A^θ value derived from Eq. 1 suggests that there are no significant changes in the CAII structure due to interaction with Co^{2+} or Fe^{3+} ions when the concentration of metal ions is low. At high concentrations of Co^{2+} or Fe^{3+} ions, the positive value of δ_B^θ (Tables 2 and 4) reflect stabilization of the CAII structure. The values $p = 1$ found for both systems show the overall non-cooperativity for the interaction of Co^{2+} and Fe^{3+} ions with CAII, and include

Fig. 6 Comparison of the experimental entropies at 300 K (\blacktriangle) and 310 K (Δ) for Fe^{3+} + CAII interactions and calculated results (lines) via Eqs. 7 and 8; $\text{mmol}\cdot\text{L}^{-1}$ denotes concentrations in units or $\text{mmol}\cdot\text{L}^{-1}$



specific and non-specific interactions. These results are consistent with association equilibria resulting from specific interactions at three identical and non-interacting binding sites on CAII ($K_1 = K_2 = K_3 = 87.150 \mu\text{mol}\cdot\text{L}^{-1}$), underlying the existence of some partially unfolded intermediate forms of CAII that form Co^{2+} + CAII and Fe^{3+} + CAII complexes. The positive values of δ_B^θ imply that specific interactions, defined here as preferential interactions between Co^{2+} or Fe^{3+} ions and the native folded state of CAII, are present and dominant. The δ_B^θ values suggest that Co^{2+} and Fe^{3+} ions play important roles in the folding of the CAII molecule. Values of δ_B^θ for the Fe^{3+} + CAII complex are larger than those of Co^{2+} + CAII (Tables 2 and 4), implying that the stability of Fe^{3+} + CAII complexes is greater than for Co^{2+} + CAII complexes. In Co^{2+} + CAII and Fe^{3+} + CAII interactions, either the chemical bonds become stronger or chemical bonds are being formed throughout the interactions that result in negative ΔH values. At the same time, this act of forming or even strengthening of a bond restricts the movement of the molecule (its ability to rotate, vibrate, etc.) and hence decreases the CAII molecule's entropy. The relatively small negative ΔG values (Figs. 2 and 5) are consistent with the above interpretations. Carbonic anhydrase is a metalloenzyme containing Zn^{2+} . This metal, which is involved in the biologically active site, can be removed and replaced with other bivalent metal ions. When Co^{2+} is substituted for the native Zn^{2+} , the enzyme activity is substantially preserved [13], which is in agreement with our results.

Open Access This article is distributed under the terms of the Creative Commons Attribution Noncommercial License which permits any noncommercial use, distribution, and reproduction in any medium, provided the original author(s) and source are credited.

References

1. Orioli, P.: Structural studies on the interactions between metal ions and biological molecules. *Croat. Chem. Acta* **71**, 659–672 (1998)

2. Barrese, A.A., Caroli Genis, S., Zoe, F.: Inhibition of carbonic anhydrase II by thioxolone: a mechanistic and structural study. *Biochemistry* **47**, 3174–3184 (2008)
3. Sarraf, N.S., Saboury, A.A., Ranjbar, B., Moosavi-Movahedi, A.A.: Structural and functional changes of bovine carbonic anhydrase as a consequence of temperature. *Acta Biochim. Polonica* **51**, 665–671 (2004)
4. Selma, I., Sinan, S., Cakir, U., Bulut, M., Arslan, O., Ozensoy, O.: In vitro inhibition of cytosolic carbonic anhydrases I and II by some new dihydroxycoumarin compounds. *J. Enzyme Inhib. Med. Chem.* **23**, 32–36 (2008)
5. Bertini, I., Lanini, G., Luchinat, C.: Equilibrium species in cobalt(II) carbonic anhydrase. *J. Am. Chem. Soc.* **105**, 5116–5118 (1983)
6. Nyman, P.O., Strid, L., Westermark, G.: Carboxyl-terminal region of human and bovine erythrocyte carbonic anhydrases. *Eur. J. Biochem.* **6**, 172–189 (2005)
7. Winum, J.Y., Rami, M., Montero, J.L., Scozzafava, A., Supuran, C.T.: Carbonic anhydrase IX: a new druggable target for the design of antitumor agents. *Med. Res. Rev.* **28**, 445–463 (2007)
8. Rezaei Behbehani, G., Waghorne, E.W.: A high-performance theory for thermodynamic study of solvation in mixed solvents. *Thermochim. Acta* **478**, 1–5 (2008)
9. Rezaei Behbehani, G., Saboury, A.A., Bagheri, A.F.: A Thermodynamic study on the binding of calcium ion with myelin basic protein. *J. Solution Chem.* **36**, 1311–1320 (2007)
10. Rezaei Behbehani, G., Saboury, A.A., Taleshi, E.: A comparative study of the direct calorimetric determination of the denaturation enthalpy for lysozyme in sodium dodecyl sulfate and dodecyltrimethylammonium bromide solutions. *J. Solution Chem.* **37**, 619–629 (2008)
11. Rezaei Behbehani, G., Saboury, A.A., Taleshi, E.: Determination of partial unfolding enthalpy for lysozyme upon interaction with dodecyltrimethylammoniumbromide using an extended solvation model. *J. Mol. Recognit.* **21**, 132–135 (2008)
12. Rezaei-Behbehani, G., Saboury, A.A., Gheibi, N.: A new approach for thermodynamic study on binding some metal ions with human growth hormone. *J. Solution Chem.* **37**, 1645–1655 (2008)
13. Bertini, I., Luchinat, C., Scozzafava, A.: Interaction of cobalt(II) bovine carbonic anhydrase with aniline, benzoate and anthranilate. *J. Am. Chem. Soc.* **99**, 581–584 (1977)